Electron-impact ionization of O^{q+} ions for $q=1-4$

S. D. Loch, J. Colgan, and M. S. Pindzola
Department of Physics, Auburn University, Auburn, Alabama 36849

M. Westermann, F. Scheuermann, K. Aichele, D. Hathiramani, and E. Salzborn
Institut für Kernphysik, University of Giessen, D-35392 Giessen, Germany
(Received 17 January 2003; published 25 April 2003)

Experimental measurements of the ionization cross section for O^{q+}, where $q=1-4$, performed with a crossed-beam apparatus are presented and compared with theoretical calculations. For O^{+}, the experimental measurements are in very good agreement with configuration-average time-dependent close-coupling calculations. For the remaining oxygen ions, the experimental measurements are in good agreement with time-independent distorted-wave calculations. As expected, the accuracy of the perturbative distorted-wave calculations improves with increasing ion charge.

DOI: 10.1103/PhysRevA.67.042714 PACS number(s): 34.80.Kw, 52.20.Fs

I. INTRODUCTION

The electron-impact ionization of an arbitrary atom or atomic ion continues to challenge theoretical and experimental workers. On the theoretical side, the basic direct ionization process involves two electrons escaping in a long-range Coulomb field, the three-body Coulomb problem. The ejected electron may originate in the outer shell of the atom (the most likely process from energy considerations), or, if the energy of the incoming electron is sufficient, may originate from an inner shell of the atom. Indirect ionization processes, such as excitation-autoionization, may also become important, especially for multiply charged positive ions with small numbers of valence electrons outside closed subshells. For open $2p$-shell systems, such as those studied in this paper, direct ionization is expected to dominate, although contributions from indirect ionization may become more important for higher members of the isonuclear sequence.

In recent years much progress has been made in applying nonperturbative theoretical techniques to electron-impact ionization of light atoms. For the electron-impact ionization of hydrogen, the converged close-coupling [1], the hyperspherical close-coupling [2], the *R* matrix with pseudostates [3], the exterior-complex-scaling [4], and the time-dependent close-coupling (TDCC) [5] methods are all in very good agreement with experimental measurements [6], and up to 15% lower than distorted-wave predictions [5]. Calculations for the electron-impact ionization of neutral helium using the converged close-coupling [7], the *R* matrix with pseudostates [8], and the time-dependent close-coupling [9] methods are again all in very good agreement with experimental measurements [10] and about 10% lower than distorted-wave calculations [9]. On the other hand, recent TDCC calculations on He^{+} [11] have found good agreement with convergent close-coupling calculations, distorted-wave calculations, and experiment. Good agreement has been found between the *R* matrix with pseudostates, the time-dependent close coupling, and converged close coupling for the electron-impact ionization of neutral lithium in its ground and first excited states [12], although here the three theoretical calculations are significantly lower than both distorted-wave calculations and the only available experimental measurements. The nonperturbative calculations for ionization from the first excited state of lithium are lower than the distorted-wave calculations by almost a factor of 2. However, similar calculations for electron-impact ionization of Li^{+} [13] have shown good agreement between the various nonperturbative and distorted-wave calculations and the experiment. *R*-matrix and TDCC calculations on Li^{2+} [14] have also found distorted-wave calculations to be reasonably accurate, and in good agreement with the experiment. For low-charged positive atomic ions in the Li and Na isoelectronic sequences, nonperturbative calculations have been found to be in good agreement with the distorted-wave calculations for ions with a charge of $3+$ or higher [15–24].

In comparison, there have been very few nonperturbative calculations of electron-impact ionization of open *p*-shell atoms or atomic ions. Time-dependent close-coupling calculations have been made for the electron-impact ionization of the neutral carbon and neon atoms [25]. The TDCC calculations were made using a configuration-average approximation and so did not include any explicit term-dependence in the coupling of the continuum electrons with the remaining core electrons. A useful guide to the strength of term dependent effects in electron ionization of *p*-shell atoms is to examine the largest departure from the configuration-average angular factor for the dipole exchange integral in the *LS* term of the $2p^{n}kd$ configuration. The correlation of such angular factors with term dependence in ionization cross sections has been previouly shown for Ar and Cl in the work of Griffin, Pindzola, Gorczyca, and Badnell [26]. As an example of this effect consider the ionization of neutral carbon and neon. The largest departure factor for electron ionization of carbon is $\frac{7}{15}$ in the $2pkd\,^{1}F$ term, while the largest departure factor for electron ionization of neon is $\frac{19}{15}$ in the $2pkd\,^{1}D$ term. For carbon ionization, very good agreement was found between the configuration-average TDCC calculations [25] and the experimental measurement of Brook, Harrison, and Smith *et al.* [27]. On the other hand, the configuration-average TDCC calculations [25] for neon ionization were found to be about 25% higher at the peak of the cross section than the experimental measurements of Krishnakamur and Srivastava

[28]. Since the largest departure factor for electron ionization of O^+ is $\frac{2}{5}$ in the $2p^2(^3P)kd^4P$ term, we expect to find reasonably good agreement between the TDCC calculations and the experiment.

Several experimental studies of the electron-impact ionization of oxygen ions as well as some perturbative theoretical calculations exist in the literature. Aitken and Harrison [29] measured the ionization cross section for O^+ and O^{2+}, using crossed electron-ion beams. These were among the first experimental measurements for atmospheric ions. Müller *et al.* [30] also measured cross sections for the electron-impact ionization of O^+ for a few incident electron energies, although their work was chiefly concerned with ionization of the noble gases. More recently, Yamada *et al.* [31] used a crossed-beam technique to measure the electron-impact ionization of O^+ up to 1 keV, their results being in fairly good agreement with the semiempirical prediction of the Lotz formula [32]. Donets and Ovsyannikov [33] have also made measurements of ionization cross sections for O^+ through O^{4+}.

On the theoretical side, Ganas and Green [34] used an atomic independent-particle model to compute ionization cross sections and loss functions for O^+ through O^{4+}. These calculations were in fair agreement with the existing experimental measurements at that time. Moores [35] evaluated no-exchange Coulomb-Born ionization cross sections for O^+ and O^{2+}. For O^{3+} Stingl [36] used a modified Coulomb-Born and Coulomb-Born exchange method to calculate the ionization cross section, while Pindzola *et al.* [37] used a configuration-average distorted wave approach, which was then partitioned into term resolution. Jakubowica and Moores [38] calculated the ionization cross section of O^{4+} in Coulomb-Born and distorted wave approximations in their study of lithiumlike and berylliumlike ions. Younger [39] used a distorted-wave Born approximation to calculate the electron-impact ionization of O^{4+}, in his study of ionization cross sections of the berylliumlike isoelectronic sequence.

In this paper we calculate the electron-impact ionization cross sections for O^{q+} ions, for $q=1-4$, using two different formulations of the first-order perturbative distorted-wave method. An important check on the accuracy of these distorted-wave calculations is made by performing a set of time-dependent close-coupling calculations for O^+. These sets of calculations are compared to experimental measurements made using a crossed-beam apparatus. A good agreement is found between the theoretical calculations and the experimental measurements for the ions studied here. In the following section we discuss the theoretical techniques used in these calculations. In Sec. III we present the experimental methods used in these measurements. In Sec. IV we present the comparisons between theory and the experiment for the O^{q+} ions and we conclude with a short summary.

II. THEORY

A. Time-independent distorted-wave method

The configuration-average distorted-wave expression for the direct ionization cross section of the $(n_t l_t)^{w_t}$ subshell of any atom is given by [40]

$$\sigma=\frac{32w_t}{k_i^3}\int_0^{E/2}\frac{d(k_e^2/2)}{k_e k_f}\sum_{l_i,l_e,l_f}(2l_i+1)(2l_e+1)\times(2l_f+1)\mathcal{P}(l_i,l_e,l_f,k_i,k_e,k_f), \tag{1}$$

where the linear momenta (k_i,k_e,k_f) and the angular momentum quantum numbers (l_i,l_e,l_f) correspond to the incoming, ejected, and outgoing electron, respectively. The total energy $E=k_i^2/2-I=k_e^2/2+k_f^2/2$, where I is the subshell ionization energy. The first-order scattering probability is given by [40]

$$\begin{aligned}\mathcal{P}(l_i,l_e,l_f,k_i,k_e,k_f)&=\sum_\lambda A^\lambda_{l_i,l_e,l_f}[R^\lambda(k_e l_e,k_f l_f,n_t l_t,k_i l_i)]^2\\&+\sum_{\lambda'} B^{\lambda'}_{l_i,l_e,l_f}[R^{\lambda'}(k_f l_f,k_e l_e,n_t l_t,k_i l_i)]^2\\&+\sum_\lambda\sum_{\lambda'} C^{\lambda,\lambda'}_{l_i,l_e,l_f}R^\lambda(k_e l_e,k_f l_f,n_t l_t,k_i l_i)\\&\times R^{\lambda'}(k_f l_f,k_e l_e,n_t l_t,k_i l_i),\end{aligned} \tag{2}$$

where the angular coefficients A,B,C may be expressed in terms of standard $3-j$ and $6-j$ symbols and R^λ are standard radial Slater integrals.

The radial distorted-waves $P_{kl}(r)$ needed to evaluate the Slater integrals are solutions to a radial Schrödinger equation given by

$$\left(h(r)-\frac{k^2}{2}\right)P_{kl}(r)=0, \tag{3}$$

where

$$h(r)=-\frac{1}{2}\frac{d^2}{dr^2}+\frac{l(l+1)}{2r^2}-\frac{Z}{r}+V_D(r)+V_X(r), \tag{4}$$

and Z is the atomic number. The direct V_D potential is given by

$$V_D(r)=\sum_u^{\text{occ}} w_u\int_0^\infty\frac{P^2_{n_u l_u}(r')}{\max(r',r)}dr', \tag{5}$$

where $P_{n_u l_u}(r)$ are the configuration-average Hartree-Fock bound radial orbitals [41]. The exchange V_X potential is calculated in a local density approximation [42]. The incident and scattered electron continuum orbitals are evaluated in a V^N potential, while the ejected continuum orbital is calculated in a V^{N-1} potential [39], where $N=\Sigma_u w_u$ is the total number of target electrons. These calculations are listed as DWIS(N) (distorted wave, incident and scattered electrons in V^N potential) in the following sections. The DWIS(N) method has proved especially accurate for high angular momentum scattering. A second set of calculations was also made where the incident, scattered, and ejected electrons were calculated in a V^{N-1} potential [43], listed as

DWIS($N-1$) in subsequent sections. This method is generally more accurate for low angular momentum scattering. The continuum normalization for all distorted waves is one times a sine function.

B. Time-dependent close-coupling theory

The configuration-average time-dependent close-coupling expression for the direct ionization of the $(n_t l_t)^{w_t}$ subshell of any atom is given by [5,14,25]

$$\sigma = \frac{w_t \pi}{4(2l_t+1)k_i^2} \int_0^E \frac{d(k_e^2/2)}{k_e k_f} \sum_{l_i,l_e,l_f} \sum_{L,S} (2L+1) \times (2S+1)\mathcal{P}(l_i,l_e,l_f,L,S,k_i,k_e,k_f), \tag{6}$$

where L is the angular momentum quantum number obtained by coupling l_t and l_i (or l_e and l_f) and S is the spin momentum quantum number obtained by coupling two spin-$\frac{1}{2}$ electrons. The scattering probability is obtained by projecting the two-dimensional radial wave function $P^{LS}_{l_1 l_2}(r_1,r_2,t)$ onto appropriate products of bound and continuum radial orbitals at a suitable time after the collision.

The radial wave functions $P^{LS}_{l_1 l_2}(r_1,r_2,t)$ are solutions to the time-dependent radial Schrödinger equation given by

$$i\frac{\partial P^{LS}_{l_1 l_2}(r_1,r_2,t)}{\partial t} = T_{l_1 l_2}(r_1,r_2) P^{LS}_{l_1 l_2}(r_1,r_2,t) + \sum_{l_1',l_2'} U^{L}_{l_1 l_2, l_1' l_2'}(r_1,r_2) P^{LS}_{l_1' l_2'}(r_1,r_2,t), \tag{7}$$

where the expressions for the quantities $T_{l_1 l_2}(r_1,r_2)$ and $U^{L}_{l_1 l_2, l_1' l_2'}(r_1,r_2)$ can be found in Ref. [25]. The radial wave function at a time $t=T$ following the collision is obtained by propagating the time-dependent close-coupling equations on a two-dimensional finite lattice. The two-electron wave functions fully describe the correlation between the ejected and scattered electrons at all times following the collision.

The bound and continuum radial orbitals required to describe the initial state and the projection can be obtained by diagonalization of the Hamiltonian $h(r)$ of Eq. (4) on a one-dimensional finite lattice. The direct V_D and local exchange V_X potentials are constructed as pseudopotentials in which the inner nodes of the valence Hartree-Fock orbitals are removed in a smooth manner. This prevents unphysical excitation of filled subshells during time propagation of the close-coupled equations [17]. The Fourier transform method [14], used to extract the ionization cross section for many incident electron energies for only one time propagation of the Schrödinger equation, is employed to obtain cross sections over a wide range of energies around the peak of the ionization cross sections for O^+.

III. EXPERIMENTAL METHOD

The measurements were performed at the Giessen electron-ion crossed-beam setup, which has been described in detail earlier [44,45]. In order to produce oxygen ions we fed carbon dioxide into the plasma of a 10-GHz electron cyclotron resonance ion source [46]. With this method stable ion currents of about 20 nA (O^{4+}) up to about 200 nA (O^+) could be obtained at an acceleration voltage of 10 kV. For O^{4+} we used the isotope ^{18}O instead of ^{16}O because $^{16}O^{4+}$ has the same mass to charge ratio as $^{12}C^{3+}$. After magnetic separation of the desired ion species and tight collimation to a typical diameter of 2 mm, the ion beam was crossed perpendicularly with an intense electron beam. We used a high current electron gun designed by Becker *et al.* [47] for all cross section measurements in the electron energy range from threshold up to 1 keV. This gun delivers a ribbon-shaped beam and an electron current of up to 450 mA at 1 keV. After the interaction the ionization products were separated magnetically from the incident ion beam and detected by a single particle detector. The primary ion beam was collected in a large Faraday cup. To obtain absolute cross sections the dynamic crossed-beam technique was employed [48] where the electron gun and thus the electron beam is moved mechanically up and down across the ion beam with simultaneous registration of the ionization signal, the electron and the ion current. Measurement times for one data point range from 50 s to about 2000 s. The total experimental uncertainties of the measured cross sections are typically 8% at the maximum, resulting from the quadrature sum of the nonstatistical errors of about 7.8% and the statistical errors at 95% confidence level.

IV. RESULTS

A. Electron-impact ionization of O^+

Distorted-wave calculations were carried out for the electron-impact ionization of O^+ over a wide range of incident electron energies. Two different distorted-wave approximations were used, as described in Sec. II. The two calculations DWIS(N) and DWIS($N-1$) are presented in Fig. 1. As a check on the accuracy of these calculations we have also carried out a series of TDCC calculations for the electron-impact ionization of O^+, from the outer $2p$ subshell, for a range of electron energies near the peak of the ionization cross section from 50 to 260 eV. As previously discussed, we employ the Fourier transform technique to obtain the cross section for many incident electron energies, for only two time propagations of the two-electron radial wave function. In these calculations a lattice extending to 102.4 a.u. was used, with a mesh spacing of 0.2 a.u. By adjusting the coefficient of the local exchange potential V_X in the construction of the pseudopotential the configuration-average ionization threshold for O^+ is tuned to 33.19 eV, which agrees with the configuration-average experimental value [49]. We note that, since we ionize out of the p subshell of O^+, three times as many angular momenta channels are coupled, due to the $l_t=1$ nature of the target.

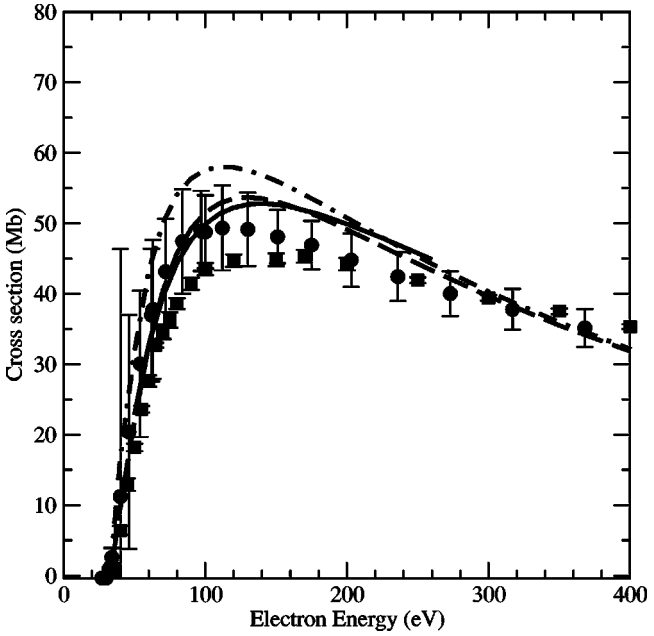

FIG. 1. Electron-impact ionization cross sections for O^+. The solid line is the time-dependent close-coupling calculation. The long-dashed line is the DWIS(N) calculation and the dot-dashed line is the DWIS($N-1$) calculation. The current experimental measurements are given by the solid circles, and the experimental measurements of Yamada *et al.* [30] are given by the solid squares ($1.0\ \text{Mb} = 1.0 \times 10^{-18}\ \text{cm}^2$).

The configuration-average time-dependent calculations were carried out for all angular momenta from $L=0$ to $L=6$, and, following our previous time-dependent calculations, our results were ''topped-up'' with distorted-wave calculations for the angular momenta above $L=6$. In these calculations we used the DWIS(N) method for our ''top-up'' since it proves more accurate for high angular momentum scattering. For both these sets of calculations the ionization cross section from the $2s$ subshell was also evaluated, using only distorted-wave methods. These have been added to the cross sections presented in Fig. 1. For this case of O^+, the excitation-autoionization cross section was found to be very small and so has not been included.

The DWIS(N) calculations are in good agreement with the time-dependent calculations for the energy range considered around the peak of the cross section. The DWIS($N-1$) calculations are consistently higher than the DWIS(N) and time-dependent calculations, although this difference is fairly small at the higher energies considered. The Coulomb-Born calculation of Moores [35] and the results of the atomic independent-particle model of Ganas and Green [34] are in surprisingly good agreement with the present TDCC calculations. In Fig. 1 we have also compared these sets of calculations to the experimental measurements made using the crossed-beam apparatus at Giessen, Germany. We find that the experimental measurements are in good agreement with the DWIS(N) and time-dependent calculations over the complete energy range considered, from near threshold to 400 eV incident electron energy. Although the calculations are slightly higher than the measurements at the peak of the cross section, the calculations are still within the error bars of the experiment. At the higher energies the agreement between the experiment and all the sets of theoretical calculations is very good. We have also compared our calculations and measurements to a previous set of experimental measurements made by Yamada *et al.* [31], also using a crossed-beam technique. Their experimental measurements are lower than both our measurements and our calculations around the peak of the cross section, although they do lie within the error bars of our experimental measurements. Again at high energy there is good agreement between all sets of measurements.

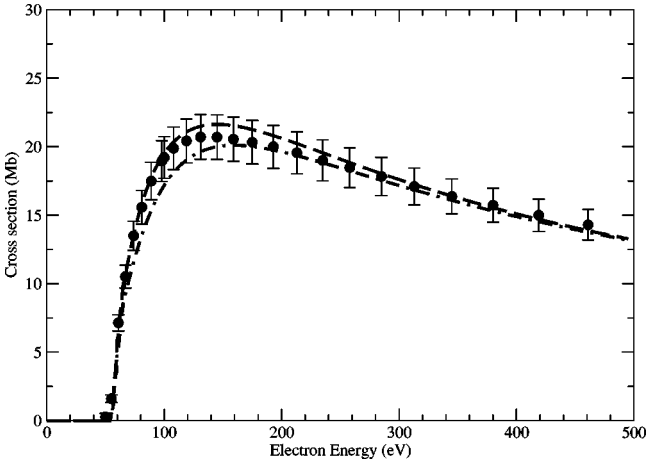

FIG. 2. Electron-impact ionization cross sections for O^{2+}. The long-dashed line is the DWIS(N) calculation and the dot-dashed line is the DWIS($N-1$) calculation. The current experimental measurements are given by the solid circles ($1.0\ \text{Mb} = 1.0 \times 10^{-18}\ \text{cm}^2$).

The good agreement between the time-dependent close-coupling calculations and the distorted-wave calculations is encouraging. Since it is well known that the accuracy of the distorted-wave calculations tends to increase with increasing charge state, we only carry out distorted-wave calculations for the remaining oxygen ion ionization cross sections.

B. Electron-impact ionization of O^{2+}

In Fig. 2 we present electron-impact ionization cross section results for O^{2+}. Again the experimental measurements are given by the solid circles. The DWIS(N) calculations are given by the long-dashed line and the DWIS($N-1$) calculations by the dot-dashed line. In these calculations the contribution from the $2p$ and $2s$ direct ionization channels has been included. There is also a small, but significant, contribution from excitation-autoionization channels. All configuration-average excitation channels from $2s-4l$ up to $2s-8l$ were included, with the most significant contributions made by excitation from $2s-4p$ and $2s-4f$ configurations.

It is clear from Fig. 2 that both sets of distorted-wave calculations are in excellent agreement with the experiment, falling within the error bars from threshold to beyond an electron energy of 500 eV. These results are higher than previous experimental measurements made by Atiken and Har-

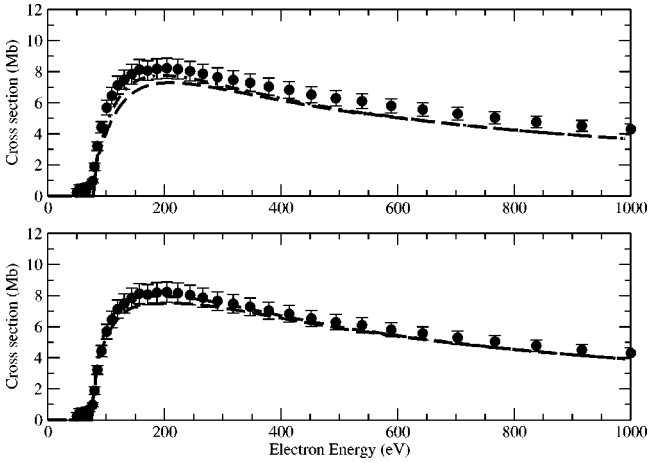

FIG. 3. Electron-impact ionization cross sections for O^{3+}, from the (a) the lowest $1s^22s^22p$ configuration and (b) the first excited $1s^22s2p^2$ configuration. The long-dashed lines are the DWIS(N) calculations and the dot-dashed lines are the DWIS($N-1$) calculations. The current experimental measurements are given by the solid circles (1.0 Mb$=1.0\times10^{-18}$ cm^2).

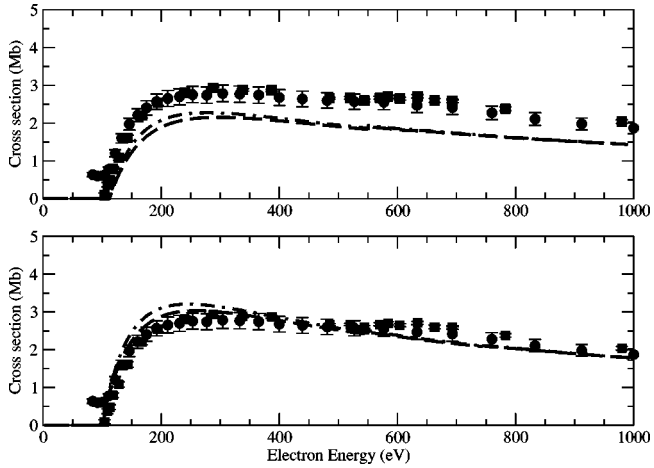

FIG. 4. Electron-impact ionization cross sections for O^{4+}, from (a) the lowest $1s^22s^2$ configuration and (b) the first excited $1s^22s2p$ configuration. The long-dashed lines are the DWIS(N) calculations and the dotted lines are the DWIS($N-1$) calculations. The current experimental measurements are given by the solid circles, and the solid squares are the experimental measurements of Falk *et al.* [45] (1.0 Mb$=1.0\times10^{-18}$ cm^2).

rison [29]. The atomic independent-particle calculation of Ganas and Green [34] for ionization from the $2p$ shell lies at slightly lower than the present results, but come into good agreement at energies above the peak of the cross section. Similarly, the Coulomb-Born results of Moores [35] for ionization from the $2s$ and $2p$ shells are lower than the present results at the peak of the cross section but agree at higher energies.

C. Electron-impact ionization of O^{3+}

We now turn to the electron-impact ionization of O^{3+}. O^{3+}, which is boronlike, has the configuration $1s^22s^22p$. However, metastable states within its first excited configuration $1s^22s2p^2$ can exist, and so it is necessary to calculate ionization cross sections from this configuration also. In Figs. 3(a) and 3(b) we present ionization cross sections from the lowest $1s^22s^22p$ and first excited $1s^22s2p^2$ configurations, respectively. Again we show our experimental measurements as well as two sets [DWIS(N) and DWIS($N-1$)] of distorted-wave calculations. For the lowest configuration of O^{3+}, the two sets of distorted-wave calculations are in good agreement with each other, with the DWIS($N-1$) calculations slightly higher at the peak of the cross section, see Fig. 3(a). As before, both sets of distorted-wave calculations include direct ionization from $2p$ and $2s$, as well as excitation-autoionization channels. The DWIS($N-1$) calculations are within the error bars of the experiment with the DWIS(N) calculations just outside.

Figure 3(b) shows the DWIS(N) and DWIS($N-1$) calculation of the ionization cross sections from the first excited configuration of O^{3+}, along with the experimental results. Again the two sets of distorted-wave calculations are in good agreement with each other. In this case, both sets of calculations are well within the error bars of the experiment. Although we get better agreement with the experiment for the distorted-wave calculations from the excited configuration, the similarity in the height and shape of the distorted wave cross sections from the ground and first excited configuration makes it difficult to determine whether there is significant metastable presence in the beam. The atomic independent-particle calculation of Ganas and Green [34] for ionization from the $2p$ subshell agrees well with the present results. The total of the term resolved distorted wave calculation of Pindzola, Griffin, Badnell, and Summers [37] agrees well with the present configuration average results. The Coulomb-Born calculation of Stingl [36] agrees with the present results at the peak of the cross section and above, but is smaller at lower energies.

We note also that significant cross section is still measured below the theoretical onset of ionization, even for ionization from the excited configuration. This may be due to the fact that our calculations are configuration averaged, and so some of the terms within this excited configuration will lie below this average value, and can contribute to the ionization cross section below the configuration-average threshold.

D. Electron-impact ionization of O^{4+}

Finally we turn to O^{4+}. Again, for this berylliumlike ion, we must consider ionization from both the lowest ($1s^22s^2$) and first excited ($1s^22s2p$) configurations, since both are likely to be present in the experimental beam. In Fig. 4 we present the current experimental measurements for O^{4+} shown by the solid circles. For this ion there are other experimental measurements with which to compare; the solid squares are measurements made by Falk *et al.* [50], using a crossed-beam technique. We see that our experimental measurements are in good agreement with the older measurements over all the energy range shown. However, we note the presence of a ''step'' in our current experimental measurements just above threshold, at around 100 eV incident electron energy. This is not the usual signature of a meta-

stable component in the beam, since the cross section does not go to zero at any point. It may be that it is due to an impurity in our ion source.

Also in Fig. 4(a) we present our two sets of theoretical calculations made using the DWIS(N) and DWIS($N-1$) methods for the electron-impact ionization of O^{4+} from the $1s^2 2s^2$ configuration. Again, the calculations contain direct ionization from both $2p$ and $2s$, as well as excitation-autoionization from $2s$. Since we now look at a larger range of energies (up to 1 keV) we also include excitation-autionization from the $1s$ orbital. This gives rise to a small ''step'' in the ionization cross section above 500 eV in both theoretical calculations. The experimental measurements also show a slight increase around this energy. Although the theoretical calculations are in good agreement with each other, they are substantially below both sets of experimental measurements. This appears to be due to the substantial metastable component in the beam. In Fig. 4(b) we present our theoretical calculations for electron-impact ionization from the excited $1s^2 2s 2p$ configuration of O^{4+}. Again the two theoretical methods are in good agreement with each other, and this time are in much better agreement with the experimental measurements. At the peak of the cross section theory is in fact higher than experiment. Since we do not know the fraction of the beam containing the excited configuration, it is difficult to precisely compare theory and experiment. $2s2p\ ^3P$ metastable presence in berylliumlike ions has historically been a problem when investigating ionization cross sections, see Falk *et al.* [50]. However, it is encouraging that the experimental measurements lie between the theoretical calculations from the ground and excited configurations. As one would expect, the present calculations agree with the previous distorted wave results of Younger [39] and Jakubowicz and Moores [38]. The atomic independent-particle results of Ganas and Green [34] are in good agreement with the present calculations near threshold, but quickly become higher than the peak of the cross section.

Note that DWIS(N) and DWIS($N-1$) calculations show closer agreement with increasing ion charge. This is to be expected as the scattering potential becomes more hydrogenic, and the differences in the V^N and V^{N-1} scattering potential seen by the incident and scattered electrons decrease for higher charge states.

V. SUMMARY

In this paper we have presented joint experimental and theoretical studies of the electron-impact ionization of O^{q+} ions, for $q=1-4$. For O^+, the experimental measurements are in good agreement with nonperturbative configuration-average time-dependent close-coupling calculations. For O^{2+} the experimental measurements are in very good agreement with two sets of perturbative configuration-average distorted-wave calculations. For O^{3+}, the experimental measurements are in good agreement with distorted-wave calculations carried out from the lowest and first excited configurations, though it is not possible to determine whether the experiment contained a significant fraction of atoms in metastable states. For O^{4+} on the other hand, it is clear that the experimental crossed-beam contains some ions in metastable states within the first excited configurations. It is not possible at this stage to determine the metastable fraction of the experimental beam but it is encouraging that the measurements lie between the two ''extreme cases'' of calculations where all the ions are in the lowest and first excited configurations, respectively.

For O^+, the good agreement between the nonperturbative time-dependent close-coupling method and the perturbative distorted-wave calculations is encouraging. Since it is well known that distorted-wave techniques tend to be more accurate for more highly charged systems (due to the more dominant nature of the nuclear potential relative to the electron correlation), the distorted-wave calculations for O^{2+}, O^{3+}, and O^{4+} should be fairly accurate. This is supported by the good agreement with the current experimental measurements.

However, from a theoretical perspective, much work remains to accurately describe, in a nonperturbative manner, electron-impact ionization from open $2p$-shell systems. As previously discussed, term dependence in the coupling of the continuum electrons with the remaining core electrons is not included in any configuration-average approximation made in time-dependent close-coupling calculations. Although this is not expected to be a major source of error in the present work, future calculations on (neutral) p-shell systems, which exhibit a significant degree of term dependence, will require an explicit description of the coupling between the continuum and core electrons. Work on this complex problem is in progress.

ACKNOWLEDGMENTS

This work was supported in part by a grant for theoretical research in plasma and fusion science (Grant No. DE-FG02-96ER54348) and a grant for scientific discovery through advanced computing (Grant No. DE-FG02-01ER54644) to Auburn University by the U.S. Department of Energy. Support by the Deutsche Forschungsgemeinschaft (DFG) is gratefully acknowledged.

[1] I. Bray and A.T. Stelbovics, Phys. Rev. Lett. **70**, 746 (1993).
[2] D. Kato and S. Watanabe, Phys. Rev. Lett. **74**, 2443 (1995).
[3] K. Bartschat and I. Bray, J. Phys. B **29**, L577 (1996).
[4] M. Baertschy, T.N. Rescigno, W.A. Isaacs, X. Li, and C.W. McCurdy, Phys. Rev. A **63**, 022712 (2001).
[5] M.S. Pindzola and F. Robicheaux, Phys. Rev. A **54**, 2142 (1996).
[6] M.B. Shah, D.S. Elliot, and H.B. Gilbody, J. Phys. B **20**, 3501 (1987).
[7] D.V. Fursa and I. Bray, Phys. Rev. A **52**, 1279 (1995).
[8] E.T. Hudson, K. Bartschat, M.P. Scott, P.G. Burke, and V.M. Burke, J. Phys. B **29**, 5513 (1996).

[9] M.S. Pindzola and F.J. Robicheaux, Phys. Rev. A **61**, 052707 (2000).
[10] R.K. Montague, M.F.A. Harrison, and A.C.H. Smith, J. Phys. B **17**, 3295 (1984).
[11] M.C. Witthoeft, M.S. Pindola, and J. Colgan, Phys. Rev. A **67**, 032713 (2003).
[12] J. Colgan, M.S. Pindzola, D.M. Mitnik, D.C. Griffin, and I. Bray, Phys. Rev. Lett. **87**, 213201 (2001).
[13] M.S. Pindzola, D.M. Mitnik, J. Colgan, and D.C. Griffin, Phys. Rev. A **61**, 052712 (2000).
[14] J. Colgan, M.S. Pindzola, and F. Robicheaux, Phys. Rev. A **66**, 012718 (2002).
[15] I. Bray, J. Phys. B **28**, L247 (1995).
[16] K. Bartschat and I. Bray, J. Phys. B **30**, L109 (1997).
[17] M.S. Pindzola, F. Robicheaux, N.R. Badnell, and T.W. Gorczyca, Phys. Rev. A **56**, 1994 (1997).
[18] K. Berrington, J. Pelan, and L. Quigley, J. Phys. B **30**, 4973 (1997).
[19] P.J. Marchalant, K. Bartschat, and I. Bray, J. Phys. B **30**, L435 (1997).
[20] O. Woitke, N. Djuric, G.H. Dunn, M.E. Bannister, A.C.H. Smith, B. Wallbank, N.R. Badnell, and M.S. Pindzola, Phys. Rev. A **58**, 4512 (1998).
[21] D.M. Mitnik, M.S. Pindzola, D.C. Griffin, and N.R. Badnell, J. Phys. B **32**, L479 (1999).
[22] M.P. Scott, H. Teng, and P.G. Burke, J. Phys. B **33**, L63 (2000).
[23] N.R. Badnell, M.S. Pindzola, I. Bray, and D.C. Griffin, J. Phys. B **31**, 911 (1998).
[24] Z. Felfli, K.A. Berrington, and A.Z. Msezane, J. Phys. B **33**, 1263 (2000).
[25] M.S. Pindzola, J. Colgan, F. Robicheaux, and D.C. Griffin, Phys. Rev. A **62**, 042705 (2000).
[26] D.C. Griffin, M.S. Pindzola, T.W. Gorczyca, and N.R. Badnell, Phys. Rev. A **51**, 2265 (1995).
[27] E. Brook, M.F.A. Harrison, and A.C.H. Smith, J. Phys. B **11**, 3115 (1978).
[28] E. Krishnakamur and S.K. Srivastava, J. Phys. B **21**, 1055 (1988).
[29] K. L Aitken and M.F.A. Harrison, J. Phys. B **4**, 1176 (1971).
[30] A. Müller, E. Salzborn, R. Frodl, R. Becker, H. Klein, and H. Winter, J. Phys. B **13**, 1877 (1980).
[31] I. Yamada, A. Danjo, T. Hirayama, A. Matsumoto, S. Ohtani, H. Suzuki, H. Tawara, T. Takayanagi, K. Wakiya, and M. Yoshino, J. Phys. Soc. Jpn. **57**, 2699 (1988).
[32] W. Lotz, Z. Phys. D **216**, 241 (1968).
[33] E.D. Donets and V.P. Ovsyannikov, Sov. Phys. JETP **53**, 466 (1981).
[34] P.S. Ganas and A.E.S. Green, J. Quant. Spectrosc. Radiat. Transf. **25**, 165 (1981).
[35] D.L. Moores, J. Phys. B **5**, 286 (1972).
[36] E. Stingl, J. Phys. B **5**, 1160 (1972).
[37] M.S. Pindzola, D.C. Griffin, N.R. Badnell, and H.P. Summers, Nucl. Fusion Suppl. **6**, 117 (1995).
[38] H. Jakubowics and D.L. Moores, J. Phys. B **14**, 3733 (1981).
[39] S.M. Younger, Phys. Rev. A **24**, 1278 (1981).
[40] M.S. Pindzola, D.C. Griffin, and C. Bottcher, in *Atomic Processes in Electron-Ion and Ion-Ion Collisions*, Vol. 145 of *NATO Advanced Study Institute, Series B: Physics* (Plenum, New York, 1986).
[41] R.D. Cowan, *The Theory of Atomic Structure and Spectra* (University of California Press, Berkeley, 1981).
[42] M.E. Riley and D.G. Truhlar, J. Chem. Phys. **63**, 2182 (1975).
[43] J. Botero and J.H. Macek, J. Phys. B **24**, L405 (1991).
[44] K. Tinschert, A. Müller, G. Hofmann, K. Huber, R. Becker, D.C. Gregory, and E. Salzborn, J. Phys. B **22**, 531 (1989).
[45] G. Hofmann, A. Müller, K. Tinschert, and E. Salzborn, Z. Phys. D: At., Mol. Clusters **16**, 113 (1990).
[46] M. Liehr, M. Schlapp, R. Trassl, G. Hofmann, M. Stenke, R. Völpel, and E. Salzborn, Nucl. Instrum. Methods Phys. Res. B **79**, 697 (1993).
[47] R. Becker, A. Müller, C. Achenbach, K. Tinschert, and E. Salzborn, Nucl. Instrum. Methods Phys. Res. B **9**, 385 (1985).
[48] A. Müller, K. Tinschert, C. Achenbach, E. Salzborn, and R. Becker, Nucl. Instrum. Methods Phys. Res. B **10/11**, 204 (1985).
[49] C.E. Moore, *Atomic Energy Levels I*, Natl. Bur. Stand. Ref. Data Ser., Natl. Bur. Stand. (U.S.) Circ. No. 35 (U.S. GPO, Washington, D.C., 1971).
[50] R.A. Falk, G. Stefani, R. Camilloni, G.H. Dunn, R.A. Phaneuf, D.C. Gregory, and D.H. Crandall, Phys. Rev. A **28**, 91 (1983).